A possible scenario for the time dependence of the multifragmentation process in Xe+Sn collisions (an explanation of the 3He puzzle)

R. Bougault, J.P. Wieleczko, M. d'Agostino, W.A. Friedman, F. Gulminelli,
N. Le Neindre, A. Chbihi, A. Le Fevre, S. Salou, M. Assenard, et al.

Lℙℂ CAEN

Sw 9739

Laboratoire de Physique Corpusculaire

ISMRA - Boulevard Maréchal Juin - 14050 CAEN CEDEX - FRANCE

A possible scenario for the time dependence of the multifragmentation process in Xe+Sn collisions (an explanation of the 3He puzzle)

R. Bougault, J.P. Wieleczko, M . D'Agostino, W.A. Freidman, F. Gulminelli, N. Leneindre, A. Chbihi,

A. Le Fèvre, S. Salou, M. Assenard, G. Auger, C.O. Bacri, E. Bisquer, F. Bocage, B. Borderie, R. Brou,

P. Buchet, J.L. Charvet, J. Colin, D. Cussol, R. Dayras, E. De Filippo, A. Demeyer, D. Doré, D. Durand,

P. Eudes, J.D. Frankland, E. Galichet, E. Genouin-Duhamel, E. Gerlic, M. Germain, D. Gourio,

D. Guinet, P. Lautesse, J.L. Laville, J.F. Lecolley, T. Lefort, R. Legrain, O. Lopez, M. Louvel, L. Nalpas,

A.D. N'guyen, J. Péter, E. Plagnol, A. Rhamani, T. Reposeur, M.F. Rivet, M. Squalli, J.C. Steckmeyer,

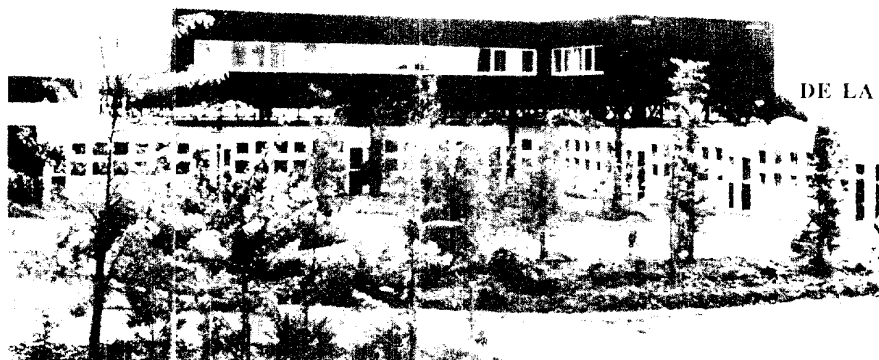M. Stern, B. Tamain, L. Tassan-Got, O. Tirel, E. Vient, C. Volant

A possible scenario for the time dependence of the multifragmentation process in Xe+Sn collisions (an explanation of the 3He puzzle)

R. Bougault[a], J.P. Wieleczko[b], M. D'Agostino[a,1], W.A. Friedman[b,2],
F. Gulminelli[a], N. Leneindre[a], A. Chbihi[b], A. Le Fèvre[b], S. Salou[b],
M. Assenard[e], G. Auger[b], C.O. Bacri[c], E. Bisquer[f], F. Bocage[a], B. Borderie[c],
R. Brou[a], P. Buchet[d], J.L. Charvet[d], J. Colin[a], D. Cussol[a], R. Dayras[d],
E. De Filippo[b], A. Demeyer[f], D. Doré[c], D. Durand[a], P. Eudes[e], J.D. Frankland[c],
E. Galichet[f], E. Genouin-Duhamel[a], E. Gerlic[f], M. Germain[e], D. Gourio[e],
D. Guinet[f], P. Lautesse[f], J.L. Laville[e], J.F. Lecolley[a], T. Lefort[a], R. Legrain[d],
O. Lopez[a], M. Louvel[a], L. Nalpas[d], A.D. N'guyen[a], J. Péter[a], E. Plagnol[c],
A. Rhamani[e], T. Reposeur[e], M.F. Rivet[c], M. Squalli[c], J.C. Steckmeyer[a], M. Stern[f],
B. Tamain[a], L. Tassan-Got[c], O. Tirel[b], E. Vient[a], C. Volant[d]

[a] **LPC Caen** (IN2P3-CNRS/ISMRA et Université) 14050 Caen cédex, France
[b] **GANIL** (DSM-CEA/IN2P3-CNRS) B.P.5027, 14021 Caen cédex, France
[c] **IPN Orsay** (IN2P3-CNRS/Université Paris Sud) B.P. 1, 91406 ORSAY cédex, France
[d] **CEN Saclay** (CEA DAPNIA/SPhN) 91191 Gif-sur-Yvette cédex, France
[e] **SUBATECH** (IN2P3-CNRS/Ecole des Mines et Université) 44072 Nantes cédex, France
[f] **IPN Lyon** (IN2P3-CNRS/Université) 69622 Villeurbanne cédex, France

[1] On leave from University of Bologna, Italy
[2] On leave from University of Wisconsin, USA

1 Introduction

The overriding goal in the study of the decay modes of excited nuclei is the determination of the laws that govern nuclear matter under conditions far away from stability. Heavy Ion collisions are a powerful tool for such investigations. They allow to create extreme states in a wide range of temperature and pressure. Numerous experimental results collected from nucleus-nucleus collisions at intermediate bombarding energy have shown that excited nuclei disintegrate predominantly into a significant number of intermediate size fragments. This fascinating process, referred as nuclear multifragmentation,

is at the focus of many experimental and theoretical works [1] since it informs on properties of excited nuclear matter at subnormal densities and could signal a liquid-gas phase transition in finite nuclear systems. In this context, exploration of central collisions of heavy systems is fundamental since it is believed that, for suitable bombarding energy, a high pressure is reached in the early stage of this kind of reactions. From such studies one expects valuable information to answer the question whether or not compression induces a specific pattern for multifragmentation. However, the understanding of the complex evolution of these collisions, from an early non-equilibrium stage to a late fragmentation stage with in between an expansion process possibly influenced by dynamical effects, remains a fantastic challenge and demands careful investigations. Above all, the fundamental issue is whether or not an equilibrated system is created in the course of the collision. This is essential to extract valid information on the thermodynamical properties of highly excited nuclear matter, and ultimately to determine its equation of state.

In a recent work [2], we have reported on the study of the multifragmentation process in central Xe+Sn collisions detected with the large acceptance 4π detector INDRA [4, 5, 6]. In this contribution, we will present our recent analysis on this set of data.

2 One source events

Let us recall the main results presented in a recent INDRA publication [2]. A first data selection is performed by imposing for each event a completeness criterion, i.e. the sum of the total detected charge exceeds 80% of the combined charge system. On this sample we have per-

formed an event by event shape analysis based on the 3-dimensional kinetic energy flow tensor calculated in the center-of-mass frame of the reaction. Only fragments with $Z \geq 3$ were included for the calculation of the tensor which is thus as much as possible independent of secondary decay effects, and gives a snapshot of the primary disintegration process. Then we have chosen as the centrality selector the value of the angle Θ_f between the beam axis and the eigenvector associated to the largest eigenvalue of the diagonalized tensor.

A selection of events with $\Theta_f \geq 60^\circ$ allows to isolate a sample where most of the charged products are isotropically emitted [3] indicating that a high degree of equilibration has been reached in the selected collisions. Indeed, an anisotropic component affects only the production of light charged particles (lcp) and the fragment ($Z \geq 3$) emission is compatible with an isotropic decay. The small number of lcp which do not participate in the source formation corresponds to a c.m forward/backward anisotropic process.

For the 50 A.MeV Xe+Sn case, the isotropic source exhausts 90% of the total detected charges. Once these numbers are corrected by the detector efficiency one obtains an estimated total charge of 90 for the isotropic source. By means of the calorimetry method applied to the isotropic component, we have estimated that the mean excitation energy of the source is about 12 A.MeV. Last, a quantitative analysis, by means of a phenomenological model, of the kinetic energy of the fragments indicates the simultaneity of the disintegration process and the need for a collective radial motion of about 2 A.MeV superimposed onto the thermal and Coulomb components.

For more details, see reference [2]. This analysis has also been applied to the 32 A.MeV

Xe+Sn system and the same conclusion about the simultaneity of the disintegration process has been found. The results are presented in table 1 for both bombarding energies.

Xe+Sn	50 A.MeV	32 A.MeV
$<E^*>$ $(A.MeV)$	12	7
$<Mimf>$	7	5.5
$<Z_s>$	81	85
$<Z_s(corrected)>$	90	95
$\sigma_{detected}$	12 mb	26 mb

Table 1: experimental measurements

The detected cross section indicated in table 1 is not corrected for detection efficiency. These results correspond to central collisions leading to the formation of a source which decays isotropically and whose size exhauts almost the whole system.

Our findings can be expressed in terms of keywords : *central collisions, single source, isotropic emission, high excitation energy, collective radial flow, multifragmentation*.

The interpretation of the results relies on the fragment characteristics only and therefore it could correspond to a specific snapshot of the disintegration process. Indeed, a unique value of 2 A.MeV collective energy fails to correctly reproduce the light charged particle average kinetic energy. In particular, the very high kinetic energy observed for ^3He [2] (reported also in [7, 8, 9] and quoted as the "^3He puzzle") remains unexplained.

In this contribution a quantitative analysis of all features of the observed multifragmenting source for the Xe+Sn reaction will be done to study the possible role of expansion in the decay patterns. The questions we want to address here are the following :

- Is equilibration achieved in the formed excited source ?

- Is the measured collective energy directly connected to compression effects or partly due to a thermal expansion ?

- Is there a unique scenario which explains the kinematical behaviour of light charged particles and fragments ?

- What is the physical origin of the extremely high energy of ^3He's observed in central collisions ?

For this purpose, we will concentrate firstly on fragment characteristics and secondly we will focus on light charged particle (lcp) properties.

3   The time evolution of the source

Since the characteristics of the fragments indicate an isotropic decay, an obvious way to deepen our understanding of the fragment emission is to compare the features of the charge distributions with predictions of a multifragmentation model. To test the statistical emission hypothesis, we have compared the experimental data with the Statistical Multifragmentation Model (SMM) [10, 11].

The fundamental assumption of the model is that a thermodynamical equilibrium is reached as the system enters the low density freeze-out region. The probabilities of the different decay channels are determined by their statistical weights. The partitions containing a fragment whose center is not contained in the fixed freeze-out volume are rejected and a microcanonical treatment of the retained partitions is performed. In a second step, secondary decays

are allowed for the primary excited fragments through evaporation, fission and Fermi break-up for light clusters. The input parameters are the freeze-out size (total number of constituents and density) and excitation energy at the freeze-out ($E^*_{freeze-out}$). Since the excitation energy is fixed, the temperature depends on the partition and is a fluctuating quantity.

In the present work, we used a modified version of the SMM-code [11] which allows a collective radial expansion at the freeze-out (E_{coll}). In this version, the hypothesis performed is a decoupling of the self-similar collective motion from the thermal one : the only effect of collective flow on the partitions is to reduce the available excitation energy ($E^*_{part} = E^*_{freeze-out} - E_{coll}$).

Calculations presented here have been performed with a freeze-out density of one third of nuclear saturation density ($E^*_{freeze-out} \equiv E^*_{1/3\rho_0}$) and simulated events were filtered with the detector acceptance and analysed as the data were.

First we performed a calculation, for the 50 A.MeV Xe+Sn system, assuming a source of Z=90 and a total excitation energy of 12 A.MeV with 2 A.MeV corresponding to a collective radial motion ($E^*_{part} = (12 - 2)\ A.MeV$). Such initial conditions are unable to reproduce the features of the elemental distribution (figure 1). The calculated bound charge and the predicted size of the biggest fragment are smaller than the measured values, and the calculated Z-distribution is steeper than the experimental one. In the framework of the statistical model a flatter Z-distribution can be observed only by decreasing E^*_{part}. This result is not surprising since the choice of the inputs used for figure 1 is consistent only with the strong - and quite irrealistic - hypothesis of an isothermal expansion from the formation of the source up to freeze-out.

Some evidence that mass and excitation energy is lost during the expansion phase can be obtained with a transport model calculation (BNV) [12]. Here, the collision is followed by solving the BNV equation with a numerical technique based on a test particle approach. The dynamics is governed by the competition between mean field effects and two body collisions. In the calculation, the nuclear part of the mean field is approximated by a density dependent Skyrme form with a compressibility modulus of 200 MeV/c, and the nucleon-nucleon cross section is assumed to be the energy, angle and isospin dependent free one. In figure 2 is presented the path in the (E, ρ) plane of the b=0 reaction for the 50 A.MeV Xe+Sn system. For this system, a source whose center coincide with the c.m is formed and its evolution in time has been extracted by considering as unbound the nucleons for which the local density is less than 1/10 of the nuclear saturation density (ρ_0). From this figure, it is possible to divide the time evolution in three stages (time t=0 corresponds here to projectile and target at contact).

- First, the compression stage : the two partners collide and the density increases. There exists in this first stage a density oscillation which corresponds to a competition between ingoing and outgoing particles during the pressure build-up (rarefaction wave). The second maximum in density is reached when the two partners are completely mixed.

- In the second stage the system starts to expand and reaches ρ_0 at around 65 fm/c (at that time the equilibrium of the system is achieved). It can be seen from the figure that from this time on the expansion is roughly isentropic.

iv

- In a third stage, at around 90 fm/c, the dilute source enters the spinodal region (which has been calculated for infinite nuclear matter).

This time evolution has to be taken into account especially because the BNV-calculation indicates a loss of mass and excitation energy of the source during the expansion phase.

Therefore the comparison with the statistical model with input parameters relying on detected information which corresponds to the whole time evolution of the source is not realistic.

4 The freeze-out condition : SMM

The SMM-model can then be used to extract the conditions of the source at the freeze-out time : mass and excitation energy. For this purpose, the experimental fragment characteristics will be compared to the model predictions. Several calculations were performed following a method similar to the one used in [13]. The size and the excitation energy at the freeze-out are determined by taking them as adjustable parameters so to reproduce at best the mean values of the fragment multiplicity, the size of the biggest fragment, and the charge bound in fragments ($Z \geq 3$). Therefore, in this procedure, we do not try to reproduce the light charged particle characteristics and we assume a unique value for the freeze-out source parameters. From the confrontation with the data, it results that SMM can reproduce the experimental static features (variables related to fragment-Z) for a source size of $Z_s(1/3\rho_0) = 78$ and $E^*_{part} = 7\ A.MeV$ (see figure 3). Indeed the agreement is spectacular. It is worthnoting that the normalisation is

done to the total number of events and not only the mean values of fragment observables are well reproduced but also the shape of their distributions. Moreover, the model predicts the observed wide spectrum of charges on several orders of magnitude. Last, the predictive power of the statistical model is also demonstrated in its ability to reproduce in great details the three body charge asymmetry distribution which quantifies the charge correlation within events. In conclusion a statistical multifragmentation model is able to quantitatively reproduce the features of the emitted fragments providing that the size and the excitation energy of the system are significantly lower than the experimental values characterizing the unique source.

The kinetic energy spectra of the fragments put a severe constraint on the model as they reflect the balance between thermal, Coulomb and eventually radial collective energy. In figure 4, we report the Z dependence of the mean values of the center of mass kinetic energy spectra of the largest fragment in each event and of the other fragments. A calculation with $Z_s(1/3\rho_0) = 78$ and $E^*_{part} = E^*_{1/3\rho_0} = 7\ A.MeV$ fails to explain the kinematic observables. A clear improvement is observed when a collective radial energy of 2.2 A.MeV is included. This value of 2.2 A.MeV is in agreement with our previous finding [2] and the SMM-calculation is now consistent with the data in absolute values and trends of both profiles.

The same procedure has been adopted for the 32 A.MeV Xe+Sn system. The results are presented in figure 5 where it can be seen that the calculation reproduces quite perfectly the selected data. As in the 50 A.MeV case, the model proves its ability to reproduce in great detail (mean values and width) a large number of observables (multiplicity of $Z \geq 3$, $Z \geq 4$,

$Z \geq 5$, $Z \geq 6$,..., three body charge asymmetry distribution, energy spectra of the different fragments,...). The "best fit" input parameters of the SMM-calculations for 50 and 32 A.MeV are summarized in table 2. The input parameters required by the statistical model corresponds to the entrance of the system in the spinodal region. A calculation based on spinodal decomposition [14] also reproduces some static observables of the fragments thus suggesting that spinodal decomposition produces statistical partitions. It will be therefore very interesting to study more exclusive variables in order to discriminate between these two approaches of disassembly at freeze-out.

SMM Xe+Sn	50 A.MeV	32 A.MeV
$E^*_{1/3\rho_0}$ $(A.MeV)$	9.2	5.5
E^*_{part} $(A.MeV)$	7	5
E_{coll} $(A.MeV)$	2.2	0.5
$Z_s(1/3\rho_0)$	78	83

Table 2: SMM calculations

We want to stress here that only with a model like SMM which is able to reproduce the experimental partitions (Z-distributions of figures 3 and 5 normalised with the number of events) it is possible to compare the extracted excitation energies (table 2) to the experimental ones measured with a calorimetric method (table 1).

In conclusion, the analysis shows that the multiple production of fragments associated to the disintegration of a single source formed in central Xe+Sn collisions at 32 and 50 A.MeV is consistent with the Statistical Multifragmentation Model. This is a strong indication that at the disintegration stage of the reaction a thermodynamical equilibrium has been reached. In the model the fragment configurations are cal-

culated first and depend on the thermal energy only, then the collective flow is introduced. This procedure is based on the assumption that thermal degrees of freedom and collective radial motion are decoupled. This decoupling hypothesis seems to agree with the data since all features of the kinematics observables together with the behaviour of the charge distribution are well reproduced.

The size and the excitation energy of the disintegrating source deduced from the analysis with SMM are lower than the experimental values. This difference may be associated to dynamical effects during the expansion phase of the system preceding the disintegration as shown by the BNV calculation. Furthermore, the question whether or not the measured collective energy is directly connected to compression effects or partly due to a thermal radial flow has still to be answered. Indeed, thermal pressure alone may account for a part of the observed flow at freeze-out. This point can be schematized in the following formula :

$$E_{coll} = E^{comp}_{coll} + E^{therm}_{coll}$$

The second contribution is due to the thermal pressure, the first one is a pure compressional energy, the sum of the two is the experimental measured value.

Finally let us remind that the measured value of E_{coll} (i.e. 2.2 A.MeV extracted from SMM-calculation for the system 50 A.MeV Xe+Sn) is a measured value at the freeze-out time. We wish also to raise the question of the time (or density) evolution of the collective energy.

5 EES model

The Expanding Emitting Source model [15] follows the time evolution of a heated nucleus. It assumes that the initial equilibrated system, once heated, expands isentropically from nuclear saturation density (ρ_0). The evolution of the system depends upon the thermal pressure which makes the nucleus expand and the nuclear forces which react against the expansion. For large temperatures, the heated nucleus will expand towards low densities, while for low temperatures the system will eventually be driven back towards ρ_0. The source emits particles and fragments during the expansion phase and the time dependent emission rates of the species are calculated within the statistical Weisskopf surface emission formalism. There is a strong coupling between the mass (A) and the density (ρ), as A decreases, ρ will decrease. Therefore the Fermi energy and the density of states will change with time. As a consequence, the temperature, defined in a Fermi gas approach, decreases during the expansion because of particle emission and change of the Fermi energy. Due to this coupling, temperature decreases more rapidly than excitation energy. When the system eventually reaches the cross-over point where the free energy for producing a free particle is equal to the free energy for producing a particle inside the volume, surface emission does not make sense any more and the model switches to volume emission. This well defined point corresponds to a density of 1/3 ρ_0 and is responsible for changes of kinematical features and for large production of Intermediate Mass Fragments (IMF) which are not copiously produced in the surface emission phase. The EES-model thus clearly considers two freeze-out conditions. The first one, the entropy freeze-out condition, is taken at nuclear saturation density (ρ_0), the second one, called the "force-freeze-out" condition is set to 1/3 ρ_0. When considering microscopic calculations, presented in figure 2 for BNV, up to the spinodal region where in the framework of fluctuations a mean-field calculation looses its validity, we see that the entropy is saturated around ρ_0 which corresponds to achieved equilibrium (entropy freeze-out condition) while the isentropic expansion phase puts the nucleus in the spinodal region at around 1/3 ρ_0 which could be considered as the "force-freeze-out" condition of the EES-model.

We have performed EES-calculations for the 50 A.MeV Xe+Sn system. The input values for the EES calculations are the measured ones (A=214, Z=90, E*=12 A.MeV) and ρ_0 is taken as the initial density. Due to technical reasons, only fragments with Z$\leq$10 are considered in the model.

First we have performed a standard calculation. In this case the expansion is governed by thermal pressure alone. In such conditions, the system expands towards low densities without stopping meaning that at 12 A.MeV excitation energy no density build-up is a priori needed to explain the occurence of multifragmentation. The whole process yields numerous IMF with charge $\leq$10 with a mean multiplicity compatible with the experimental one when considering the same range for the charge. In figure 6, we compare the calculated (labelled 0 A.MeV) and measured mean kinetic energy of the differents elements. One observes a clear underestimation. This excludes a purely thermal origin for the collective motion observed in the data. As a matter of fact, the standard calculation, with no collective energy at ρ_0, gives $E_{coll} = 0.5\ A.MeV$ at 1/3 ρ_0.

Then another calculation was performed as-

suming a collective radial energy stored in the initial system at ρ_0. This collective radial energy at ρ_0 can be here considered as a pure compression effect since it assumes implicitly that the source was formed at a density greater than ρ_0. This compression energy reduces the thermal excitation energy of the source since in the calculation the total excitation energy is kept to be 12 A.MeV. For this calculation, we still observe an expansion towards low densities without stopping, but the duration of the whole process is shortened. Taking as initial collective value (compression energy) the one extracted from the SMM-calculation improves the agreement but the calculated values still underestimate the data (figure 6). Last a slight increase to 2.5 A.MeV mean compression energy agrees with the data (figure 6). With such a value at ρ_0 the model predicts a residual collective energy of about 2.3 A.MeV at 1/3 ρ_0 in good agreement with the value obtained with SMM. The results are summarized in table 3. In this table is also presented the time interval of the expansion phase between the two freeze-out conditions. We do see the effect of an initial compression energy at ρ_0 which shortens the process.

$E_{coll}^{comp}(\rho = \rho_0)$	$E_{coll}(\rho = 1/3\rho_0)$	Δt
0 A.MeV	0.5 A.MeV	60 fm/c
2.5 A.MeV	2.3 A.MeV	35 fm/c

Table 3: EES model

In conclusion, in this chapter we have shown that the measured collective energy in 50 A.MeV Xe+Sn collisions corresponds to compression effects.

An interesting piece of information about our EES-calculations concerns the isospin degree of freedom. Between the two freeze-out conditions, i.e. during the expansion from ρ_0 to 1/3 ρ_0, the isospin of the source is conserved. This result shows the specificity of multifragmentation studies which cannot be interpreted with a low bombarding energy mentality, i.e. surface emission from a compound nucleus at ρ_0, but rather contain a new and specific physics concerning dilute systems.

6 SMM, EES and BNV calculations

Due to the evolutionary nature of the EES-modelization, global properties of the system such as size, density, collective energy can easily be followed during the process. When looking at the characteristics of the system given by EES-calculation at the "force-freeze-out" point (1/3 ρ_0), we found them pretty close to the freeze-out conditions deduced from the SMM-calculation (table 4).

50 A.MeV Xe+Sn	SMM	EES
$E^*_{1/3\rho_0}$ (A.MeV)	9.2	10.3
E_{coll} (A.MeV)	2.2	2.3
$Z_s(1/3\rho_0)$	78	74

Table 4: characteristics of the source at 1/3 ρ_0

In order to have a global understanding of the multifragmentation process, we can now come back to the BNV-calculation presented before for the 50 A.MeV Xe+Sn b=0 reaction. In figure 7, is presented the evolution of the collective energy, the maximum density (value calculated in the center of the source) and the degree of equilibration of the source as a function of time. Here the collective energy is the mean radial part of the total kinetic energy per nucleon.

The t=0 time is taken when the two reaction partners are in contact. We see, as already discussed, two maxima in the density profile. At about 65 fm/c the system reaches ρ_0 and equilibrium. Since the mean-field tends to restore nuclear media towards normal density (i.e. nuclear saturation density), about at the same time the collective energy reaches its maximum value. The value given by the BNV-calculation, around 2.5 MeV/A at ρ_0, is in agreement with the one extracted from the EES-calculation. At about 90 fm/c, the system enters the spinodal region with a reduced collective energy of about 2 A.MeV pretty close to the one deduced from EES and SMM calculations. If one thinks that at that point fluctuations increasingly develop, then our BNV-calculation does not give the correct subsequent behaviour because in the spinodal region a mean-field calculation looses its validity. The spinodal curve is here calculated for infinite nuclear matter which makes this statement only qualitative. Anyhow, we do see that the time interval from ρ_0 to $1/3$ ρ_0 is compatible with the EES-calculation (table 3).

To conclude, the time evolution of the multifragmentation process cannot be neglected. From our analysis with the 50 A.MeV Xe+Sn system, the formed compressed source (Z=90, E^*=12 A.MeV) in central reaction expands and reaches the freeze-out point with modified characteristics concerning size and excitation energy. The loss in size corresponds to about 15%. The emission during the expansion phase concerns mostly light particle and therefore does not rule out our SMM-analysis based on fragment characteristics. The loss in excitation energy is about 20%. The measured collective energy at freeze-out corresponds to about 90% of the maximum compression energy achieved.

The loss in mass and excitation energy explains clearly why the characteristics of the light charged particles are different from those of the fragments. The fragments trigger the freeze-out while the lcp characteristics are the result of the different phases of the multifragmentation process.

7 The light charged particles

We shall now focus on light charged particles (lcp) detected in coincidence with fragments in the set of data selected. The analysis is restricted to the isotropic contribution by selecting only lcp emitted between 70° and 110° in the center of mass (perpendicular emission around 90°). The angular range is chosen so to guarantee that the lcp's are emitted from the source. The anisotropic lcp-component, not discussed here, is forward/backward peaked.

In figure 8, we present the mean kinetic energy of light charged particles detected around 90 degrees c.m for 32 and 50 A.MeV Xe+Sn. The prediction of the multifragmentation model SMM is also presented in figure 8 for both bombarding energies and for input parameters which reproduce the fragment characteristics (table 2). In the SMM-model lcp's originate from the freeze-out configuration or from secondary decay of primary clusters. We see that, apart from alpha-particles, the reproduction of experimental mean energies is poor. This is the same conclusion as in our previous work [2] where experimental data were compared to the result of a phenomenological model which only includes secondary decay processes for lcp production. In particular, the very high mean energy of ^{3}He is not reproduced by the statistical model and this figure is an experimental example of the "^{3}He puzzle" reported also in [7, 8, 9].

In order to take into account the time evolution of the multifragmentation process, we have calculated the lcp's mean energies within the EES model. The input parameters of the model are those which lead to agreement with the fragment characteristics for the system 50 A.MeV Xe+Sn. The result is presented in figure 9. A general qualitative agreement is achieved. The mean energy of Z=2 particles are reproduced, and especially the ^{3}He puzzle does not seem to be a puzzle any more. The good agreement is due to the occurrence of particle emission during the expansion phase. This can be understood from figure 10. Here are presented the cumulative yields of tritons, alpha-particles and ^{3}He. It should be underlined that each cumulative yield is independent and normalized to the yield at t=80 fm/c. Therefore any multiplicity comparison between the different species cannot be extracted from this figure. The first 35 fm/c correspond to the surface emission phase (emission during expansion) and at 35 fm/c the system reach the "force-freeze-out" point where volume emission sets in. Alpha-particles are mostly emitted in the second phase, and in that sense they could be considered as small fragments since they behave roughly in the same way (about 20% of $3 \leq Z \leq 10$-fragments are emitted during the expansion phase). For ^{3}He, the situation is completely reversed : 70% of them are produced by surface emission. The triton case is a situation in between. This explains why the statistical model SMM is unable to reproduce the mean energy of lcp except for alpha-particles which are mostly emitted after the freeze-out point (i.e. after 35 fm/c).

Going back to the data concerning lcp mean kinetic energy presented in figure 9, (i) we explain the difference between alpha-particles and ^{3}He by the multiple origins of alpha-particles (expansion phase, freeze-out process, secondary decays) as compared to an almost unique origin of ^{3}He (emission during the expansion phase), (ii) we explain the difference between ^{3}He and tritons by the Coulomb barrier. Both particles have roughly the same binding energy but ^{3}He's are preferentially emitted at high temperatures in order to overcome the Coulomb barrier. More precisely, ^{3}He's are mostly forbidden after the expansion phase because of Coulomb effects rather than preferentially emitted during the expansion phase.

This explanation of the ^{3}He-puzzle is based on a model calculation. We will now present experimental results which indicate that this qualitative statement seems to be correct. In figure 11, invariant c.m velocity distributions are presented for tritons and ^{3}He detected around 90° and for the two sets of data (32 and 50 A.MeV). This representation enhances the low velocity component. At 32 A.MeV and for the two species, the distribution can be interpreted by two contributions. A weak low velocity component and a high velocity one for which a Coulomb effect is present. Increasing the bombarding energy we see that the weight of the low velocity component is enhanced for tritons. For ^{3}He the low velocity contribution remains very weak indicating a dominant emission process with a large Coulomb effect for both bombarding energies. When we compare with the EES-prediction which reproduces the IMF characteristics, figure 11 for ^{3}He, a qualitative agreement is obtained. The high velocity part of the distribution corresponds to surface emission during the expansion phase and the low velocity contribution corresponds to emission after the "force freeze-out" point of the EES-model. We recall that this representation enhances the low velocity part since the surface emission in figure 11-bottom corresponds to 70%

x

of ^{3}He produced by EES-model. This last point, when looking to ^{3}He-data, could signify that almost all the detected ^{3}He are produced during the expansion phase.

From the EES-calculation presented in figure 11, we can argue that when we consider A=3-particles having a c.m velocity greater than 6 cm/ns we retain species emitted during the expansion phase. This fact can be verified with the recorded data. In figure 12 are presented the c.m energy spectra of tritons and ^{3}He detected around 90° for 50 A.MeV Xe+Sn. For low c.m energies, there exists large differences between the two spectra. Nevertheless at large energies the slopes seem identical. In order to get a deeper insight, we present in figure 12-bottom the ratio between the two spectra as a function of the c.m energy. For c.m energies greater than 50 MeV, the ratio is constant and exactly equal to 1.38, the N/Z ratio of the formed compressed source (this value of 1.38 is the N/Z ratio for Xe, for Sn and for Xe+Sn, therefore the hypothesis of considering 1.38 to be the N/Z of the formed compressed source is realistic). This remarkable fact has to be compared to EES-predictions for which surface emission is dominant for A=3 c.m energies greater than about 50 MeV. The value of 1.38 reached by the ^{3}H/^{3}He ratio, which corresponds to the N/Z of the source, can be explained by first chance emission or coalescence for high energy particle production.

As a conclusion of this chapter, we think that we have demonstrated that the characteristics of the light charged particles can be explained by taking into account particle emission during the expansion phase. It is only by unfolding the different emission steps that one can conciliate the kinetic information from both lcp and fragments. The "^{3}He puzzle" can be explained if one considers that almost all of them are emitted during the expansion phase. This point, confirmed by our experimental observations, can lead to experimental measurements of the beginning of the expansion phase since ^{3}He can be considered as early messengers of the multifragmentation process therefore probing the very first instants of the dynamical expansion.

8 Conclusion

In this paper we did not try to describe in detail the mechanism of fragment formation at freeze-out (statistical disassembly or spinodal decomposition), we refer to [14] for this point. Rather we tried to describe the time evolution of the multifragmentation process. In conclusion, because we have well characterized the source and its disintegration process, we think that we have given an answer to the following questions :

- Is equilibration achieved in the formed excited source ? *yes* for the dilute system which leads to fragment production (disassembly stage).

- Is the measured collective energy directly connected to compression effects or partly due to a thermal expansion ? *we have measured a genuine compression energy.* In the framework of a model, the measured collective energy corresponds to 2.5 A.MeV compression energy at nuclear saturation density for 50 A.MeV bombarding energy. This value, confirmed by transport model calculation, corresponds to a density in the center of the source of about 1.3 ρ_0.

- Is there a unique scenario which explains the kinematical behaviour of light charged particles and fragments ? *yes*, by taking

into account the time evolution of the multi-fragmentation process (emission during the expansion phase).

- What is the physical origin of the extremely high energy of ^3He's observed in central collisions ? ^{3}He's bear information about the dynamical process since they are mostly forbidden after the expansion phase. Therefore they are peculiar light charged particles. They could probe the very first instants of the dynamical process which leads to the disassembly of the dilute nucleus.

In order to compare the different collective energy measurements extracted from different experiments, one has to take into account the time evolution of the multifragmentation process. Within the scenario presented here, it is not surprising that collective energies measured with light charged particles are not in agreement with those extracted from fragment characteristics. Therefore ^{3}He mean energies, in our mind, are more representative of the compression energy if one wants to compare different experimental values. A tentative compilation of ^{3}He mean energies is presented in figure 13, which contains the available data from INDRA, FOPI [8] and EOS [9] collaborations. The system studied (Xe+Sn and Au+Au) present a general agreement which could directly reflect the density achieved as a function of excitation energy.

References

[1] See, for instance, L.G. Moretto and G.J. Wozniak, Annu. Rev. Nucl. Part. Sci. (1993) 379, and references quoted therein.

[2] N. Marie et al., Phys. Lett. **B391** (1997) 15.

[3] J. D. Frankland for the INDRA coll., this meeting

[4] J. Pouthas et al., Nucl. Instrum. Methods A 357 (1995) 418.

[5] J.C. Steckmeyer et al., Nucl. Instrum. Methods A 361 (1995) 472.

[6] J. Pouthas et al., Nucl. Instrum. Methods A 369 (1996) 222.

[7] K.G.R. Doss et al., Mod. Phys. Lett. **A3** (1988) 849.

[8] G. Poggi et al., Nucl. Phys. **A586** (1995) 755.

[9] M.A. Lisa et al., Phys. Rev. Lett. **75** (1995) 2662.

[10] A.S. Botvina et al., Nucl. Phys. **A475** (1987) 663.

[11] J.P. Bondorf, A.S. Botvina, A.S. Iljinov, I.N. Mishustin and K. Sneppen, Phys. Rep. **257** (1995) 133.

[12] A. Bonasera, F. Gulminelli and J. Molitoris, Phys. Rep. **243** (1994) 1.

[13] M. D'Agostino et al., Phys. Lett. **B371** (1996) 175.

[14] M. F. Rivet for the INDRA coll., this meeting

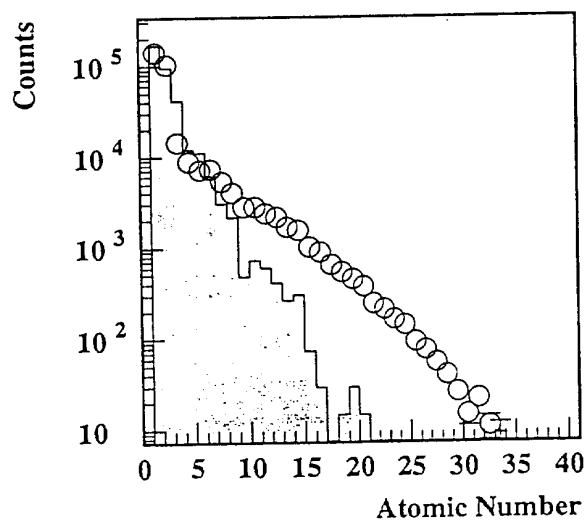[15] W. A. Friedman, Phys. Rev. **C42** (1990) 667.

Figure 1: Z-distribution for 50 A.MeV Xe+Sn one source events : the circles are the data, the histogram corresponds to SMM prediction for a source of Z=90 and of total excitation energy of 12 A.MeV (10 A.MeV to generate the partitions and 2 A.MeV of collective radial energy).
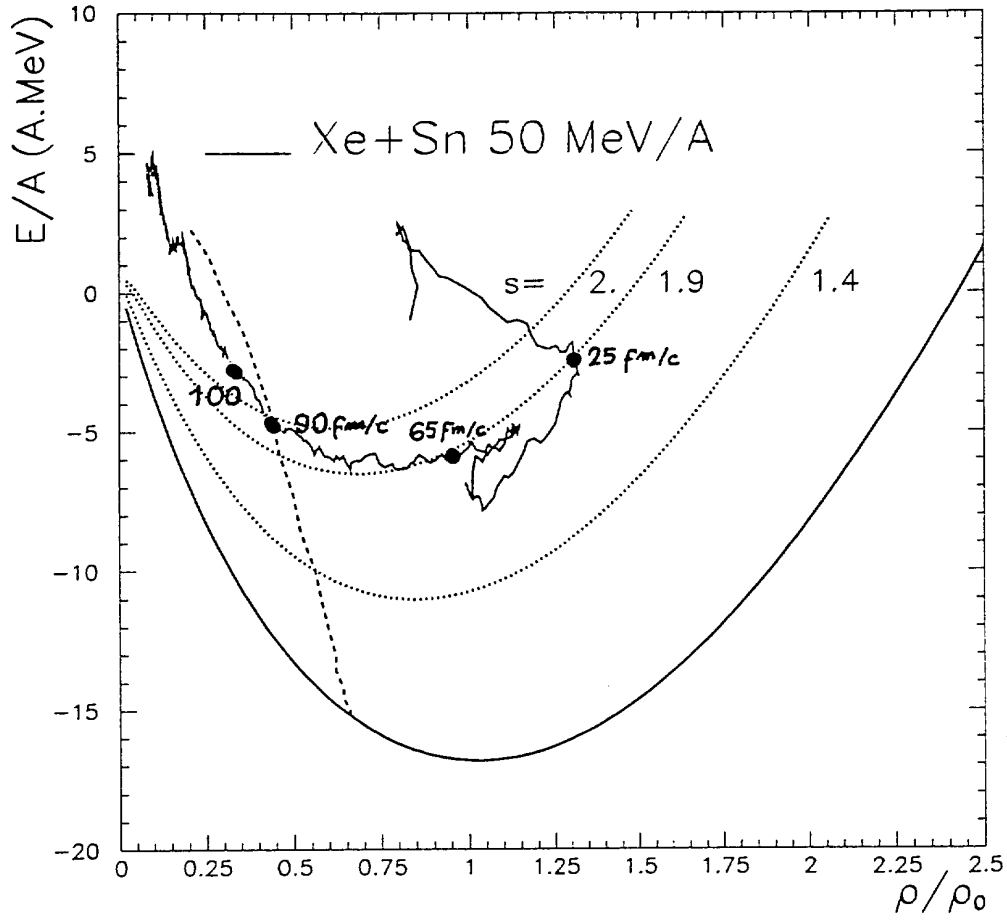
Figure 2: BNV prediction for 50 A.MeV b=0 reaction : path in the (energy,density) plane. The time evolution is indicated from projectile and target at contact (t=0). Four isentropic lines are presented and the limit of the spinodal region is delineated by a dashed line.
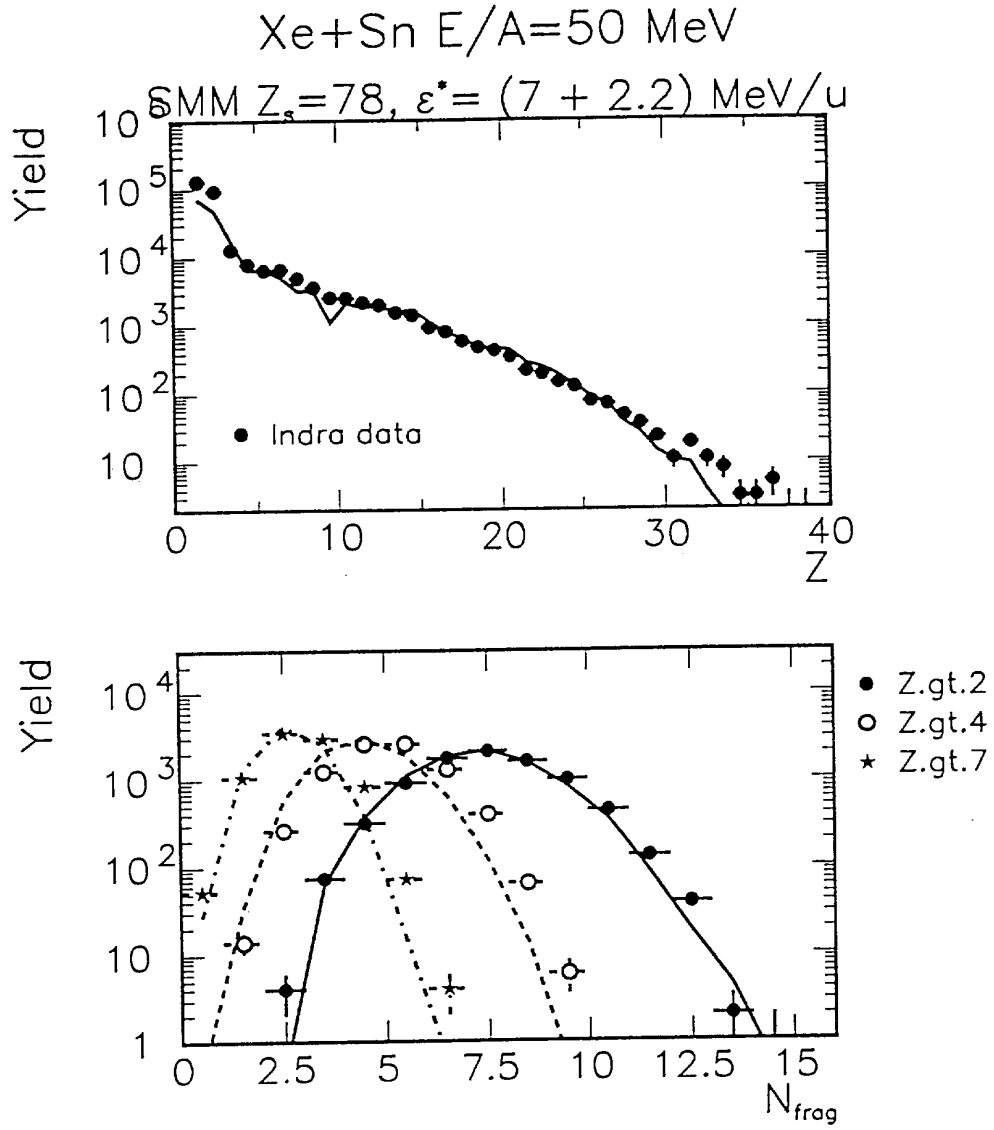
Figure 3: SMM and 50 A.MeV Xe+Sn data : result of the procedure described in the text. The lines are SMM-predictions, the points are the data. On the bottom figure are presented the multiplicity of fragments for different low thresholds in atomic number.
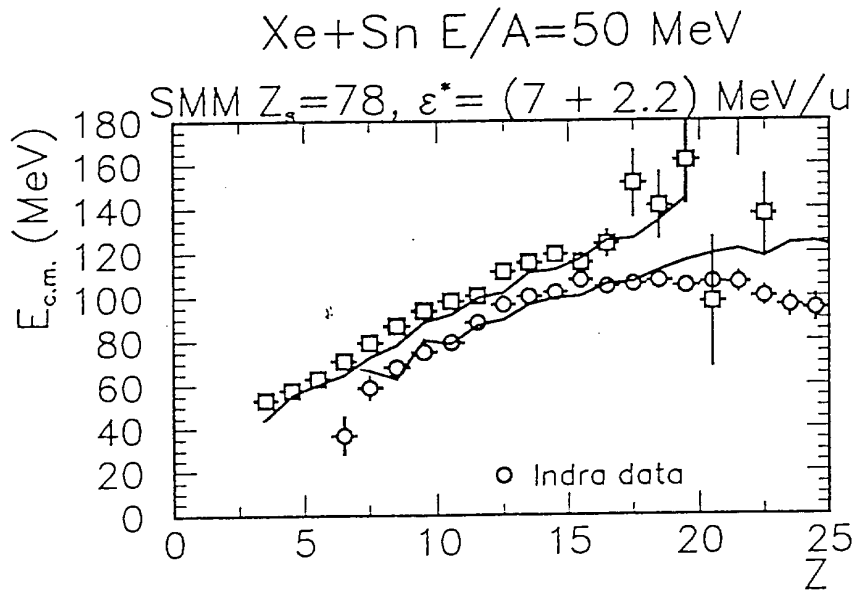
Figure 4: SMM and 50 A.MeV Xe+Sn data : mean kinetic energy in the center of mass of the different elements. The lines are SMM-predictions, the points are data. The fragments have been sorted in two categories, largest fragment in each event (circle) and all but the largest fragment in each event (square).
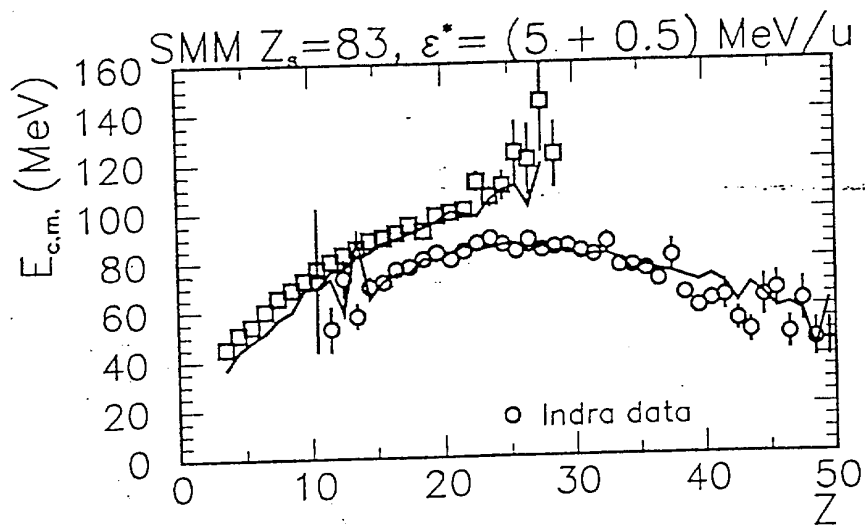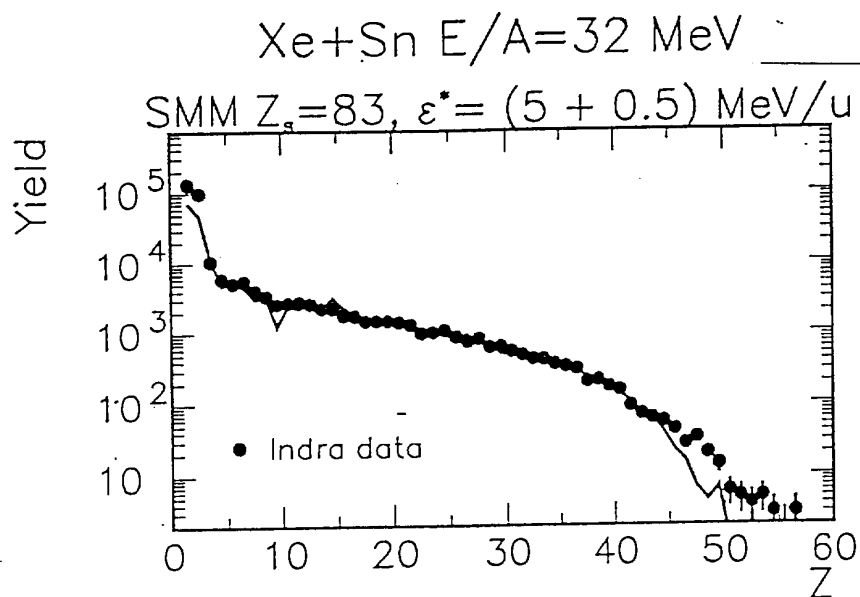
Figure 5: SMM and 32 A.MeV Xe+Sn data : The lines are SMM-predictions, the points are data. The sorting in two categories of fragments for the bottom picture is described in the previous figure.
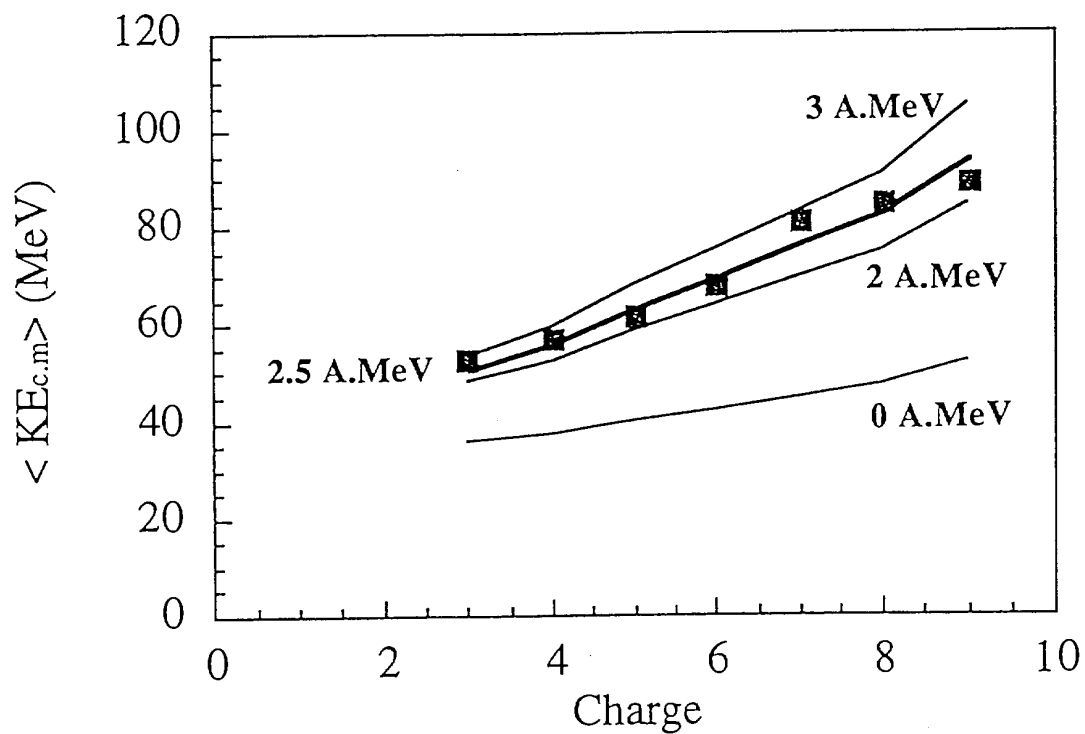
Figure 6: EES and 50 A.MeV Xe+Sn data : mean kinetic energy in the center of mass of the different elements (Z≤10). The lines are EES-predictions, the points are data. The "0 A.MeV" line corresponds to a pure thermal expansion. The other lines correspond to a compression energy at normal density of 2, 2.5, 3 A.MeV.
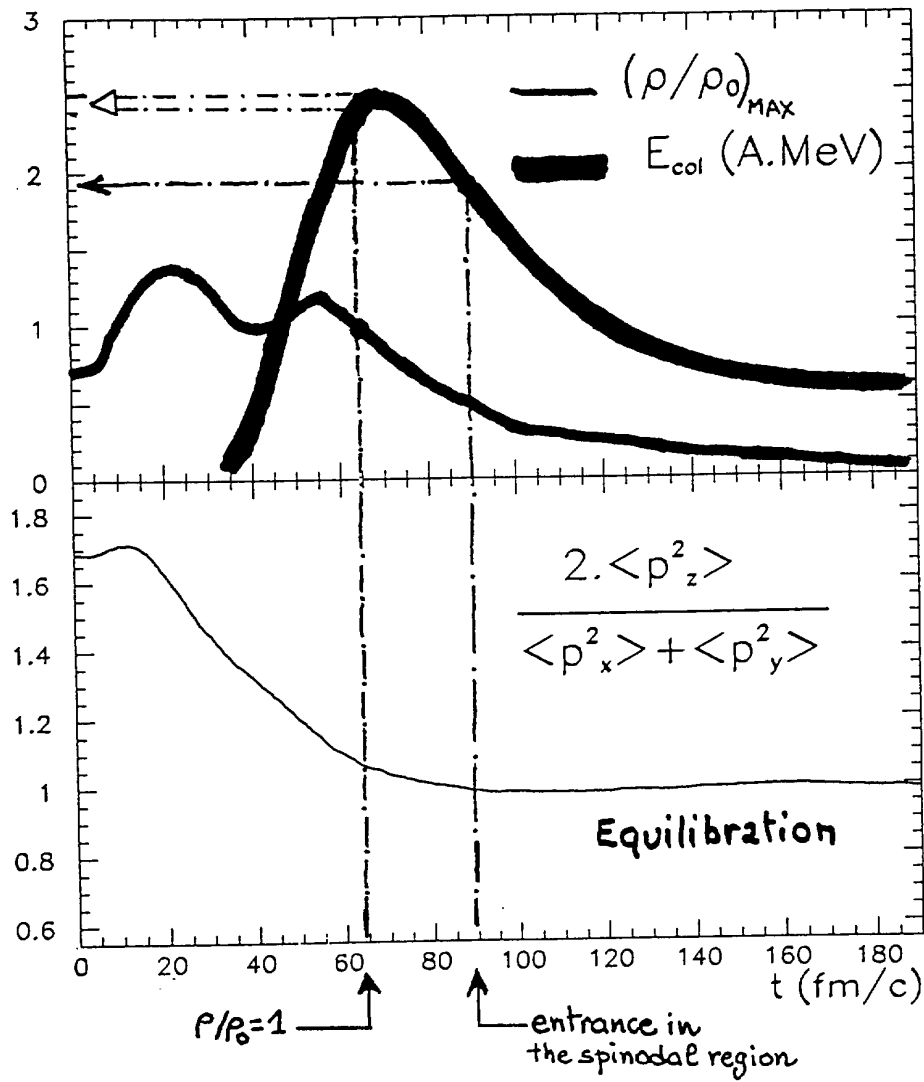
Figure 7: BNV calculation for b=0 Xe+Sn 50 A.MeV : density, collective energy and degree of equilibration are presented as a function of time (t=0 for projectile and target at contact).
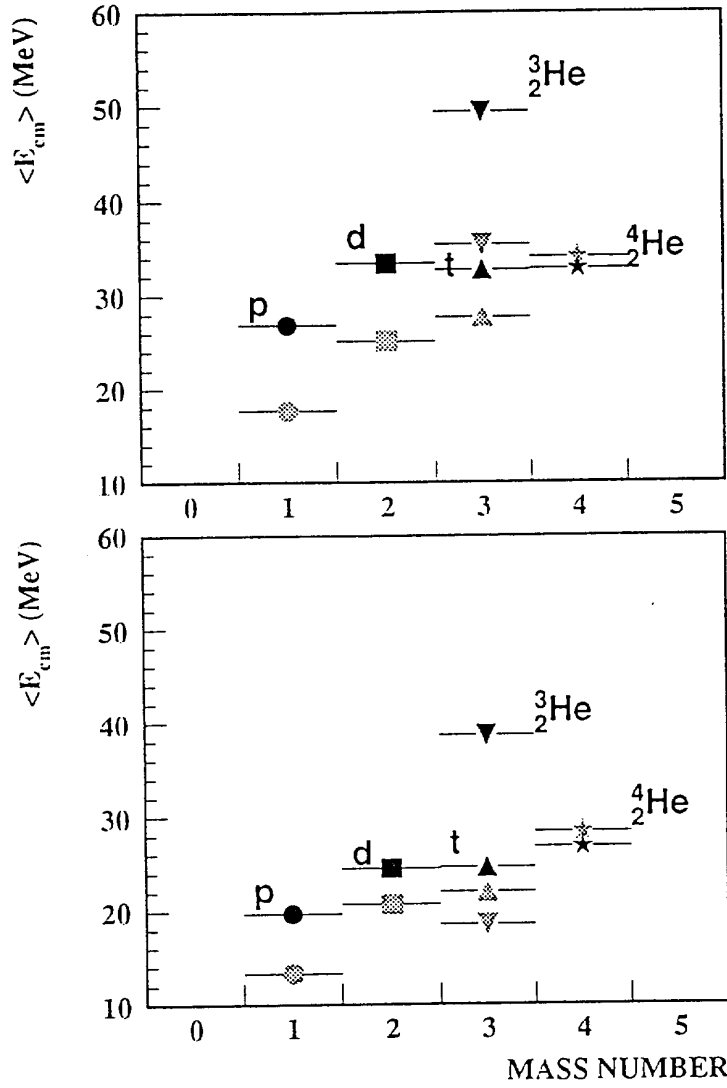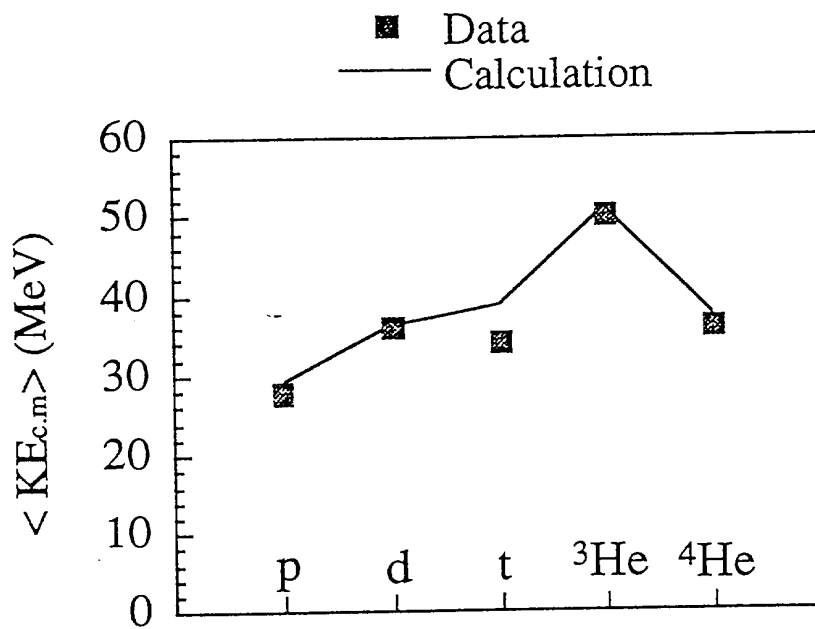
Figure 8: SMM and light charged particles for 50 and 32 A.MeV Xe+Sn : average c.m kinetic energy of the light charged particles (black points are data) for a perpendicular emission ($70° \le \Theta_{cm} \le 110°$) in the center of mass. The result of the SMM-calculation which reproduces the associated fragment characteristics is shown (grey points). The upper picture corresponds to the 50 A.MeV case, the bottom one is for 32 A.MeV.

Figure 9: EES and light charged particles for 50 Xe+Sn : average c.m kinetic energy of the light charged particles (black squares are data) for a perpendicular emission ($70° \leq \Theta_{cm} \leq 110°$) in the center of mass. The result of the EES-calculation which reproduces the associated fragment characteristics is shown (line).

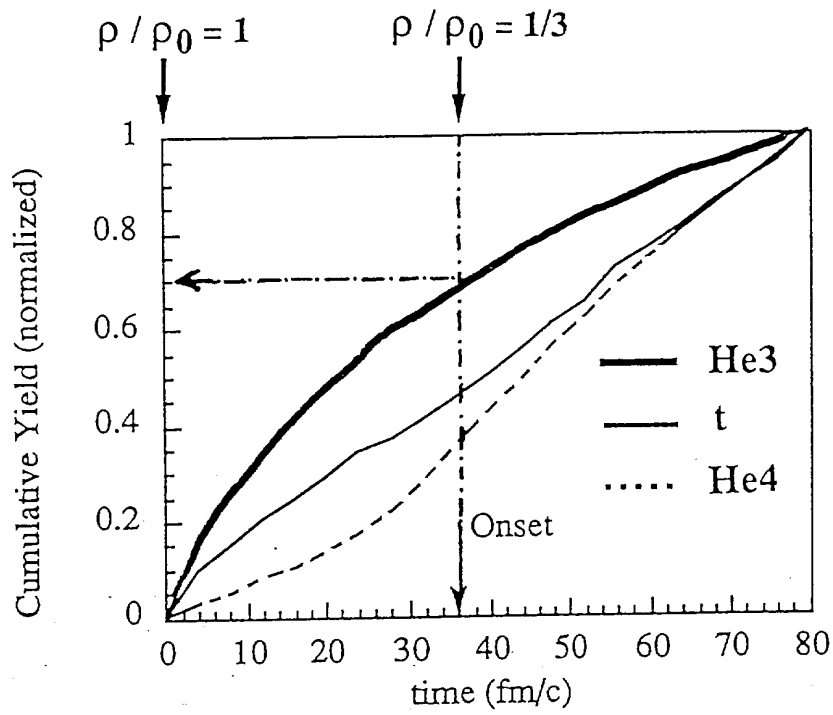$$\text{C.Y.(time)} = \frac{1}{Y} \int_{0}^{\text{time}} \frac{dY}{dt} \, dt$$

Figure 10: EES-calculation : cumulative yield for ^{4}He, ^{3}He and triton production. The first 35 fm/c corresponds to surface emission during the expansion phase.
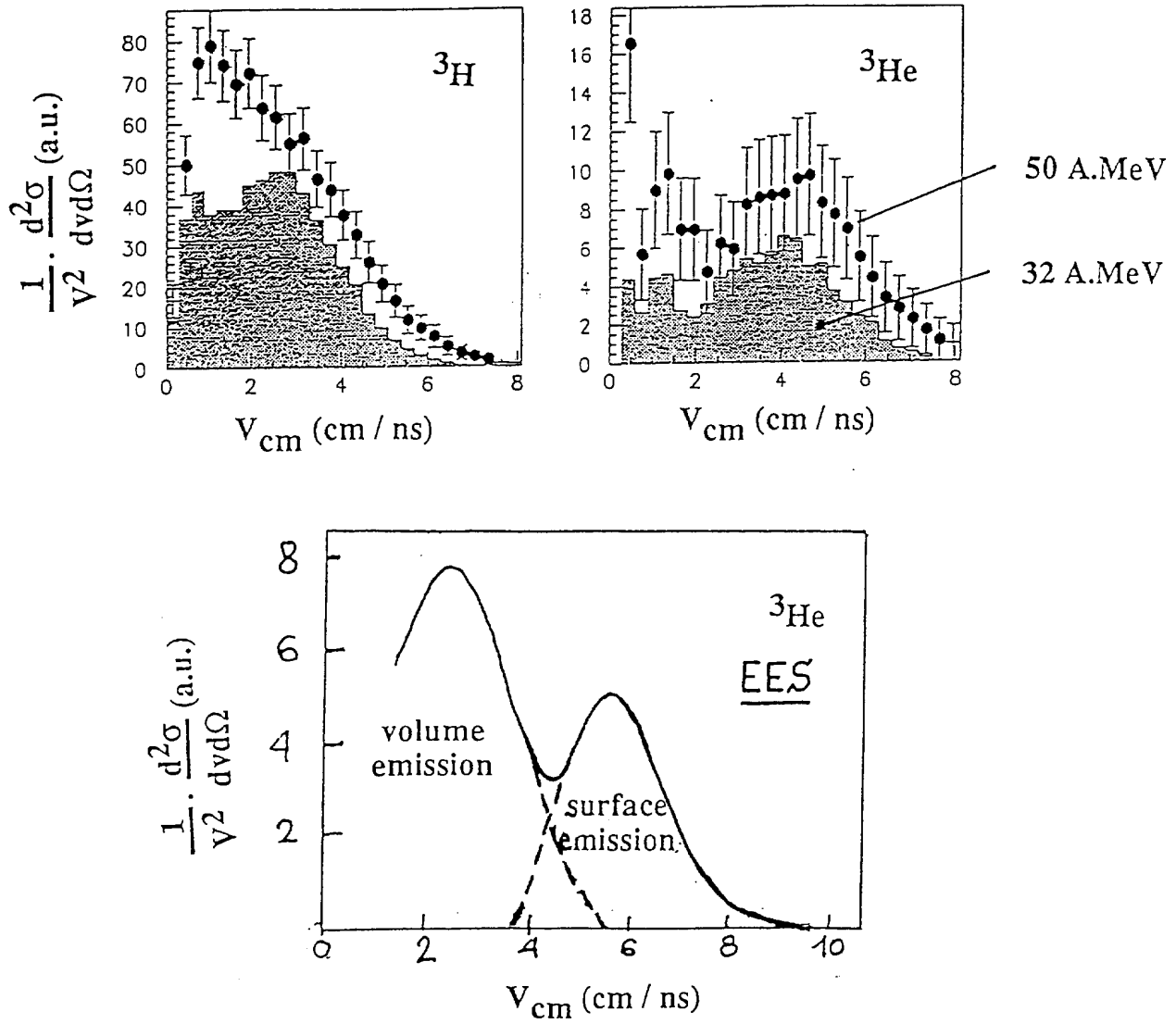
Figure 11: Invariant velocity distributions for tritons and ^{3}He : the top pictures are data for 32 and 50 A.MeV Xe+Sn, the bottom corresponds to EES-calculation for ^{3}He production at 50 A.MeV.
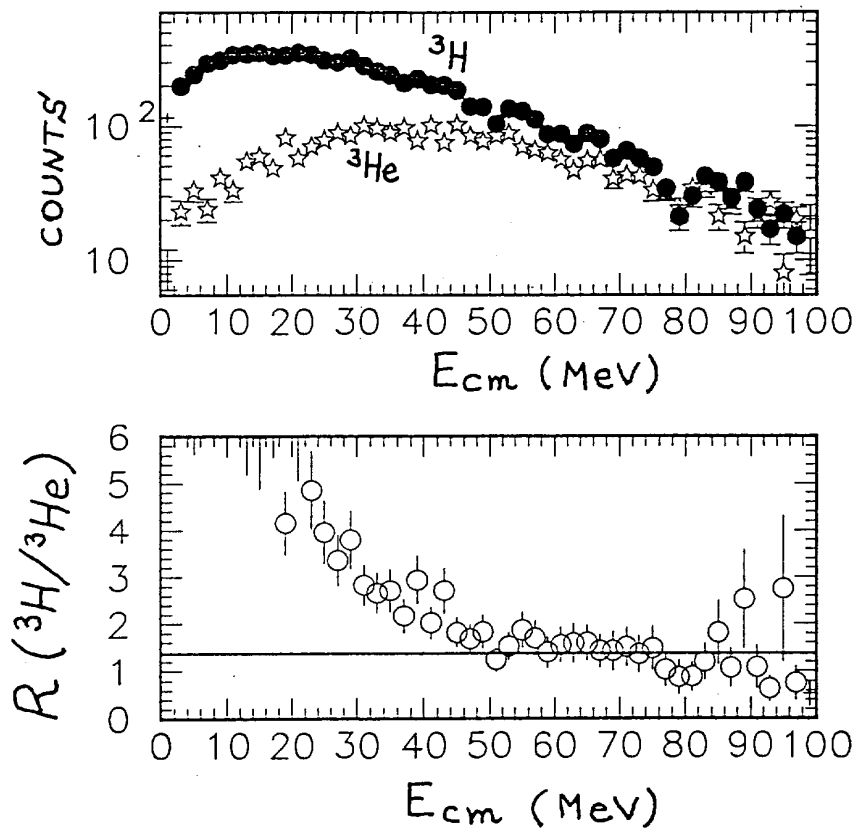
Figure 12: 50 A.MeV Xe+Sn data : the top picture is c.m energy spectra for tritons and ^{3}He, the bottom is the ratio of the two energy spectra. The line for the bottom picture corresponds to the N/Z ratio of the source.

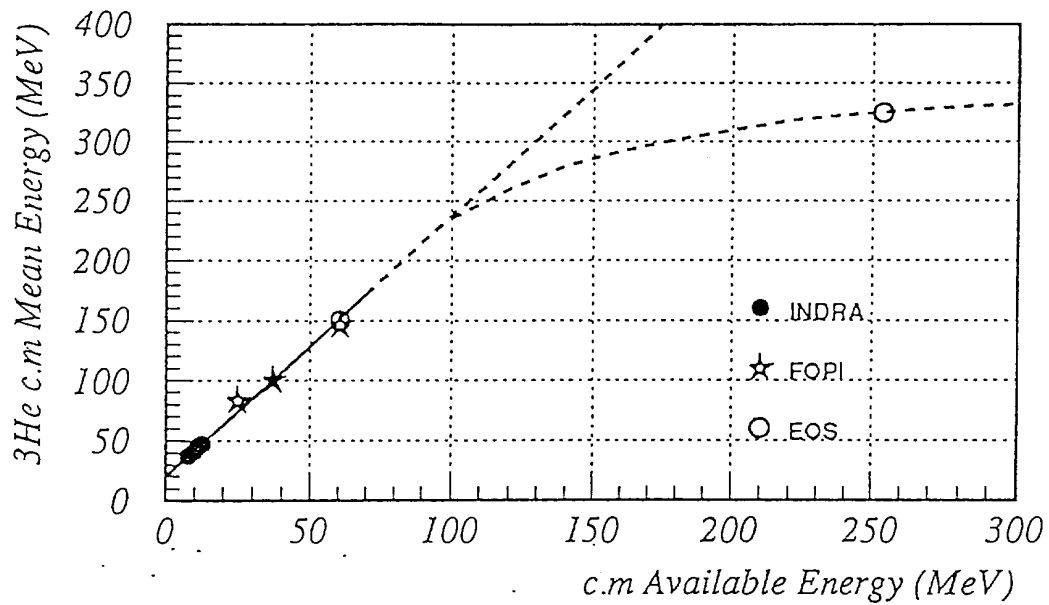Figure 13: Central collisions and symmetric systems : average center of mass kinetic energy of ^3He detected at c.m 90° as a function of available energy in the c.m (i.e. excitation energy). The mean kinetic energy of ^3He reflects the achieved density of the formed source. The variation is first linear with excitation energy. While the bombarding energy approaches the onset of particle production (as π) this linear behaviour is broken indicating a less efficient energy deposition in the participant zone.